Research Article ISSN 2832-9384

Journal of Materials and Polymer Science

An Investigation on the Effect of Various Coagents on the Peroxide Degradation of Polypropylene

Justin Bulten[1*], **Francesco Picchioni**[1] **and Roberta Cipullo**[2]

[1]*University of Groningen, Netherlands.*

[2]*Federico II University of Naples, Italy.*

***Corresponding author**

Justin Bulten
University of Groningen,
Netherlands.

Submitted : 20 Feb 2024 ; Published : 21 Mar 2024

Citation: Bulten, J. et al. (2024). An Investigation on the Effect of Various Coagents on the Peroxide Degradation of Polypropylene. J mate poly sci, 4(1):1-21.

Abstract

The peroxide degradation of polypropylene was studied in supercritical carbon dioxide in the presence of a coagent. 18 coagents were tested and their results were analysed to gain insight on structure-property relations. Broadly four different categories were identified, where coagents such as toluene do not show much of an effect, molecules such as hydroquinone show a large effect towards suppressing the degradation, and molecules such as phenol are somewhere in the middle. The fourth category was only based on a single molecule, n-hydroxyphthalimide, which was the only molecule to exhibit more degradation than the peroxide would have done alone.

Keywords: Polypropylene, degradation, β-scission, structure-property relations, peroxide, n-hydroxyphtalimide, hydroquinone, benzoquinone, phenol, toluene, supercritical carbon dioxide.

Introduction

Conventional Ziegler-Natta catalysts produce polypropylene (PP) in a highly isotactic fashion, with a high molecular weight (MW typically in the range of 100-400 kDa) and a high polydispersity index (PDI, around 5-7). However, certain applications perform considerably better when the PP chains are shorter and more uniform in length (e.g., injection moulding). In other words, a reduction in both MW and PDI is much desired. It is rather fortuitous, therefore, that PP is susceptible to a process known as β-scission. Due to the relative stability of a tertiary carbon radical centre, the hydrogen atom on the methine side is abstractable. A simple radical initiator, such as those derived from a peroxide scission, will do.

On the other hand, there are also instances where PP degradation is undesired, or partially desired. For instance, PP needs to have a higher melt strength if it has to be made into a polymer film. One way to improve this is by long chain branching (LCB-PP, or HMS-PP) (Huovinen et al., 1997; Scheve et al., 1998). The first step in accomplishing this is to break one chain, and have the broken parts reattach to another chain. Therefore, degradation is partially desired because it is the first step, but a subsequent step has to take place. If the desire is to functionalize the PP-backbone, then degradation is likely a competing reaction, which makes it undesirable (Dorscht & Tzoganakis, 2002; Liu et al., 2005; Oromiehie et al., 2014).

The β-scission step is extremely fast. It is, in fact, so fast that many models of such reactions assume it to be instantaneous while still obtaining models that agree with the experimental results (Berzin et al., 2000; Iedema et al., 2001; Tzoganakis et al., 1989). As such, this method has become a convenient way to reduce MW. On top of that, since the longer chains have a higher chance of getting affected, for the simple reason that they carry more methine groups per chain, longer chains are broken down more often compared to shorter chains; therefore, the PDI also decreases. It is these attributes that have awarded β-scission a relevant position in the polymer industry, where it's usually referred to as controlled degradation or peroxide shifting.

However, the control of β-scission is somewhat limited. First of all because peroxide initiators work through a stoichiometric scheme. Once they have abstracted a hydrogen, they will be bound to it irreversibly, thus losing the ability to abstract another and commence another β-scission step. Thus, further breakdown of the chains requires more peroxide to be added, but this has an adversarial side effect, since a large presence of radical initiator makes it increasingly likely for the initiator to irreversibly graft onto the chain instead of taking a hydrogen away from it (akin to reaction 7b in Scheme 2) or to induce side reactions due to "cage effects" (Brown et al., 1962). For this reason, an increase in peroxide concentration causes the extent of the process to plateau, since it negates two radical initiators to have the desired effect:

1. The initiator itself is no longer able to abstract a hydrogen, and so it will not lead to scission.
2. It could graft onto a position where a previous initiator had taken a hydrogen, thus stabilizing a spot that was primed for β-scission (Tzoganakis et al., 1989).

Fortunately, there are ways around this limitation. One simply being a cascading process, where a small amount of peroxide is added incrementally along the way, thus keeping the concentration of radical initiators low. Another would be to select a different peroxide with a longer half-life time, which would also lead to a lower concentration. However, both these steps require longer residence times, which makes the process more time consuming than desired, or perhaps even unfeasible.

A third way would be to introduce a coagent that has a reversible element. It would, as it were, have a catalysing effect on the process; i.e., partaking in the process but not being consumed by it. There exists a variety of compounds that have such competences, and they can be divided into categories. For each category, the key is stabilization of the radical mechanism to assess the effect of each coagent. The structures of the coagents used in this work are presented in Table 1.

There exists a variety of positions within organic compounds that can play host to a radical with relative ease because they are stabilized by neighbouring groups. There are 2 systems to stabilize compounds, but quite some molecules apply a combination of systems.

1. Electronegativity, the inherent affection of an atom towards electron density, where the radical is stabilized through hyper conjugation or the induction effect with neighbouring groups, of which the tertiary carbon is a common example.
2. π-conjugation, either the benzylic position, where the radical is stabilized by the delocalized electrons of the aromatic ring, or the allylic position, where the radical is stabilized by an adjacent C=C double bond.

$scCO_2$

Supercritical carbon dioxide ($scCO_2$) is an upcoming technology that is highly interesting to replace volatile organic compounds (VOCs) as a solvent in chemical synthesis. CO_2 is non-flammable and non-toxic – and, therefore, harmless – which is advantageous because CO_2 is a gas at ambient conditions – and, therefore, $scCO_2$ is also rather volatile. Furthermore, it is abundant – and, therefore, cheap – and has a relatively mild critical point – and, therefore, operational costs will also be low.

Polymerization processes have been demonstrated to be successful in $scCO_2$ (Picchioni, 2014). However, as the molecular weight increases, the solubility decreases substantially, which makes post-polymerization processes less eligible. However, certain aspects such as initiator decomposition remain the same, and the effects in low-viscous environments are enhanced.

Post-polymeriziation processes also have potentially to gain from the switch to $scCO_2$. At high MW, the viscosity is high, and solubility is not entropically favoured. In these systems, $scCO_2$ might have a plasticising effect which makes mass-transfer much easier. It would be interesting to see what the effect of $scCO_2$ is. The solubility in PP ranges from about 20-260 g-CO_2/kg-PP in a range of 5-25 MPa and 313-483 K (Lei et al., 2007; Sato et al., 1999). The conditions used in this work would result in a solubility of 80 g-CO_2/kg-PP.

The aim of this work is to study the degradation of PP in $scCO_2$ in the presence of a coagent. The effect of each coagent is analysed to place the coagents into categories. The objective here is to look for correlations between chemical structures and behaviour, to see if structure-property relations can be estimated, which would be a powerful design tool.

The degradation is determined based on GPC, MFI, and rheology. The latter is also used to analyse possible side effects, predominantly long chain branching. To study the effects of competing reactions such as grafting, FTIR and NMR spectra were measured. A change in the chemical structure of PP would likely have repercussions in the crystallinity, which would affect the melt enthalpy, which is why DSC was performed to observe the thermal properties of the products.

Materials

The polypropylenes PP571P was obtained from Sabic petrochemicals BV, and Daploy™ WB140HMS from Borealis AG. The peroxide Trigonox 101 was received from Nouryon. N-Bromosuccinimide (99%), N-Hydroxyphthalimide (98%), endo-N-Hydroxy-5-norbornene-2,3-dicarboximide (97%), p-Xylene (99%), Phenol (99%), and Tetramethylthiuramdisulfide (97%) were purchased from Thermo Fisher Emergo B.V. The coagents Hydroquinone (99%), 2-Methylhydroquinone (99%), Benzoquinone (98%), (2,2,6,6-Tetramethylpiperidin-1-yl)oxyl (98%), Benzoic acid for Synthesis, Terephthalic Acid (98%), 3-(2-Furyl)acrylic acid (99%), tert-Butanol (>99%), Farnesene (isomer mixture), Toluene (99.5%), and α-Methyl styrene (99%) were purchased from Merck Life Science N.V. and 2,4-Diphenyl-4-methyl-1-pentene (>95%) was purchased from TCI Europe N.V. All materials were used as received

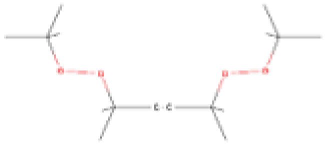 Trigonox 101	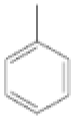 Toluene	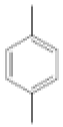 p-Xylene
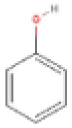 Phenol	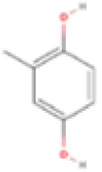 2-Methylhydroquinone	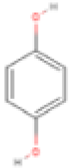 Hydroquinone
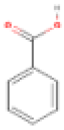 Benzoic Acid	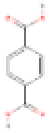 Terephthalic acid	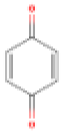 Benzoquinone
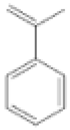 α–Methyl styrene	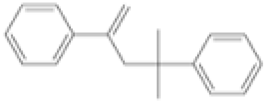 2,4-Diphenyl-4-methyl-1-pentene	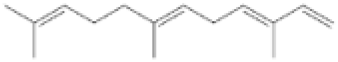 Farnesene
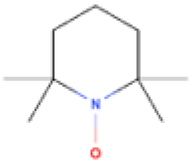 2,2,6,6-Tetramethylpiperidin-1-yl)oxyl	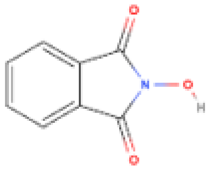 N-Hydroxyphthalimide	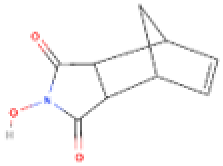 endo-N-Hydroxy-5-norbornene-2,3-dicarboximide
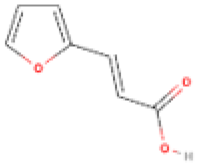 3-(2-Furyl)acrylic acid	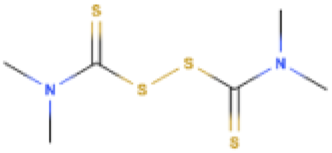 Tetramethylthiuramdisulfide	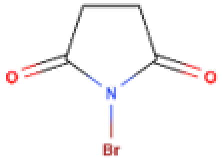 N-Bromosuccinimide

Table 1: Molecular structures used in this work

Methods

Experimental

PP, peroxide, and coagent were premixed in a glass jar and fed to a hopper. The hopper fed the mix into a 25:1 L/D twin screw extruder from Three Tec. The screw set had to be replaced due to damaged parts midway through the experiments, so a part of the experiments had to be performed with different hardware, which made them unsuitable for direct comparison. Therefore, new blank and control experiments were performed to draw a direct comparison from this new data. The barrel is made up of a feeding/transport section and five heating zones, the first of which is set to 170°C and the remaining four to 220°C. The rotating speed was set to 50 RPM, which together with a throughput of 300 g/hr leads to an average residence time of around 50 seconds. The second heating zone was equipped with an inlet of $scCO_2$, which was regulated at a flow of 7.5 g/hr ±2.5 g/hr, and a pressure of 95 bar ± 5 bar. The peroxide content was 0.1 wt%, with a molar ratio of 10:1 with each coagent. An additional experiment was done with benzoquinone, where we used 10 times as much peroxide and benzoquinone, so the peroxide content was 1 wt%, and the ratio remained 10:1. The extrudate was collected as chunks of about 1-2 cm, which were chopped into pellets of about 1-4 mm diameter and washed with acetone in a Foss Soxtec 2043 for 6 hours before being analysed.

Analysis

GPC: GPC curves were recorded with a Freeslate Rapid GPC setup, equipped with a set of two mixed-bed Agilent PLgel 10 µm columns and a Polymer Char IR4 detector using ortho-dichlorobenzene (with BHT added as a stabilizer, [BHT] = 0.4 mg mL-1). Calibration was performed with the universal method, using 10 monodisperse polystyrene samples (Mn between 1.3 and 3700 kDa). Before and after each campaign, samples from a known PP batch produced with an ansa-zirconocene catalyst were analyzed for a consistency check.

MFI: The melt flow index (MFI) was measured in a Ceast MF20 from Instron, using standard ASTM D1238, at 230°C and 2.16 kg. About 4-5 grams were inserted and preheated for 7 minutes to melt without load while the discharge die was blocked to prevent any flow during this preheating time. The die was opened at the end of the preheating time, after which followed a preheating interval with load, until a height of 46 mm was reached, and the measurement of 30 mm was started.

Rheology: The rheological frequency sweep was performed from 100 rad/s to 0.1 rad/s at 180°C to plot the viscosity over shear rate using a HR-2 Discovery Hybrid Rheometer by TA Instruments. The discs were melted and slightly pressed to ensure that the parallel plates were fully covered. Then a preheating time of 5 minutes followed to soak the discs. Then a Dynamic Strain Sweep (DSS) was performed at 100 rad/s to select the strain for the Dynamic Frequency Sweep (DFS) which was measured at the selected strain from 100 rad/s to 0.1 rad/s.

A time sweep was performed for one sample as a check for stability over time. This was done at 250°C at 3.14 rad/s for 180 seconds. This step was performed after a DSS, which covered a preheating time of 5 minutes.

FTIR: FTIR was performed using an IRTracer-100 from Shimadzu.

DSC: Differential scanning calorimetry (DSC) was performed in a DSC 25 from TA instruments. The sample is first heated to 230°C at 10 °C/ min and kept there for 5 minutes for the sample to completely melt so as to erase the thermal history. Then the sample is cooled to -50°C C at 10 °C/ min, and subsequently heated to 230°C at 10 °C/ min.

NMR: Quantitative spectra were recorded using a Bruker Advance III 400 spectrometer equipped with a high-temperature cryoprobe for 5 mm OD tubes and a robotic sample changer with preheated carousel (24 positions), on 45 mg mL-1 polymer solutions in tetrachloroethane-1,2-d_2 (with BHT added as a stabilizer, [BHT] = 0.4 mg mL-1). Acquisition conditions for ^{13}C NMR were: 45° pulse; acquisition time, 2.7 s; relaxation delay, 3.3 s; 2 K transients. Broad-band proton decoupling was achieved with a modified WALTZ16 sequence (BI_WALTZ16_32 by Bruker). The concentration of stereodefects in the isotactic fraction was obtained from the ^{13}C NMR spectra of raw samples, by measuring the fractional amount of the *mmmrrmmm* nonad in the methyl region (Busico et al., 2016; Busico & Cipullo, 2001).

Reference Values

To understand the effect of each coagent, it is important to define what happens in their absence. As such, we define 2 references. A blank sample of only PP that has been treated at the same conditions in the extruder, which is set as 0% change, and a control reference where PP has been treated at the same conditions in the presence of the peroxide at the same quantities, but without any coagent, which is set to 100% change. As such, the coagent is categorized by the degree of change compared to the blank normalized over the control.

For the MFI, the normalization was done linearly using equation 1, for the zero-shear viscosity (ZSV, determined by the Yasuda-Carreau model (Seavey et al., 2003; Wu et al., 2023)) and the M_w, the normalization was done logarithmically using equation 2.

$$\mathrm{MFI}\ (\%) = \frac{\mathrm{MFI_X} - \mathrm{MFI_{blank}}}{\mathrm{MFI_{control}} - \mathrm{MFI_{blank}}} \qquad (1)$$

$$\mathrm{ZSV}\ (\%) = \frac{\log(\mathrm{ZSV_X}) - \log(\mathrm{ZSV_{blank}})}{\log(\mathrm{ZSV_{control}}) - \log(\mathrm{ZSV_{blank}})} \qquad (2)$$

Where X is the sample, and $\mathrm{MFI_X}$ and $\mathrm{ZSV_X}$ are MFI and ZSV results of the sample.

Sample name	Coagent involved
X/Tol	Toluene
X/pXyl	p-Xylene
X/Phen	Phenol
X/meHQ	2-Methylhydroquinone
X/HQ	Hydroquinone
X/BenzA	Benzoic Acid
X/TereA	Terephthalic acid
X/BQ	Benzoquinone
X/aMS	α-Methyl styrene
X/DPMP	2,4-Diphenyl-4-methyl-1-pentene
X/Farn	Farnesene
X/TEMPO	(2,2,6,6-Tetramethylpiperidin-1-yl)oxyl
X/NHPI	N-Hydroxyphthalimide
X/NHND	endo-N-Hydroxy-5-norbornene-2,3-dicarboximide
X/FAA	3-(2-Furyl)acrylic acid
X/TMTDS	Tetramethylthiuramdisulfide
X/NBS	N-Bromosuccinimide
X/tBuOH	tert-Butanol

Table 2: Coagents with their respective sample names

Results & Discussion

Toluene

The C-H bond is usually stable enough not to be easily disrupted, making any chemical reaction unlikely, with the exception of various rates of oxidation; that is, peroxide formation, incineration, explosion, etc. In the case of saturated hydrocarbon, a C-H bond would have to be broken before any chemistry can take place. In the case of an unsaturated hydrocarbon, carrying the C=C double bond, chemistry is possible because the unsaturated group is often a functional one. However, the exception to this rule would be the aromatic ring, a circuit of a closed delocalized π-system. The aromatic ring is sufficiently stable to withstand a reaction.

Such stability can be exploited. Anything that would extend that delocalized π-system shares in the stabilization. If an aromatic ring carries a saturated side-group, the benzylic position has the potential to share in the stabilization effect, which makes it easier to disrupt the C-H bond on this position, this benzylic position. Toluene has such a C-H bond on the benzylic position; therefore, it is stabilized via system 2 as defined in the introduction.

The GPC results show a wide peak for the blank well above 100 kDa. Once the peroxide is added, the peak shifts to lower MW regions of around 100 kDa. Additionally, the peak becomes narrower and taller, to account for roughly the same area under the peak (Agilent Technologies, 2015). However, Figure 1 shows that the sample with toluene overlaps fairly well with the peroxide control and perhaps shows a little more degradation. Regardless, should the increase in degradation be judged significant, it is at least not substantial because the difference is so small that for any application this would result in practically the same properties. This might be related to the extra stabilization that renders the radical, once transferred to the toluene, not available or to side reactions of the benzylic radical. The MFI results show an index of about 10 for the blank PP. The peroxide control jumps up to around 70, with the X/Tol bar rising to roughly the same value as that of the control sample. As per the definition of the current work, those values correspond to 10 being 0%, and 70 being 100%, which again indicates that toluene does not have an influence in the process.

The rheology results show a typical shear-thinning curve for the blank. At lower frequencies, the viscosity is quite stable, where the zero-shear viscosity even has a good correlation with the MW of the polymer. As the frequency is increased, we see the viscosity dropping dramatically. The control group shows an even lower zero-shear viscosity and less shear-thinning, and the sample with toluene in turn again overlaps with the control or shows a little more degradation.

It is not surprising that the benzylic position appears to be impartial. While toluene is not used as often as a solvent for PP reactions, xylene is more widely employed. Such solution reactions tend to run at around 125-145°C for multiple hours, typically between 6 and 48 hours, and neither xylene nor toluene seems to be involved in the reaction there either (Boyron et al., 2017; Shenoy & Patil, 2010; Wang et al., 2009).

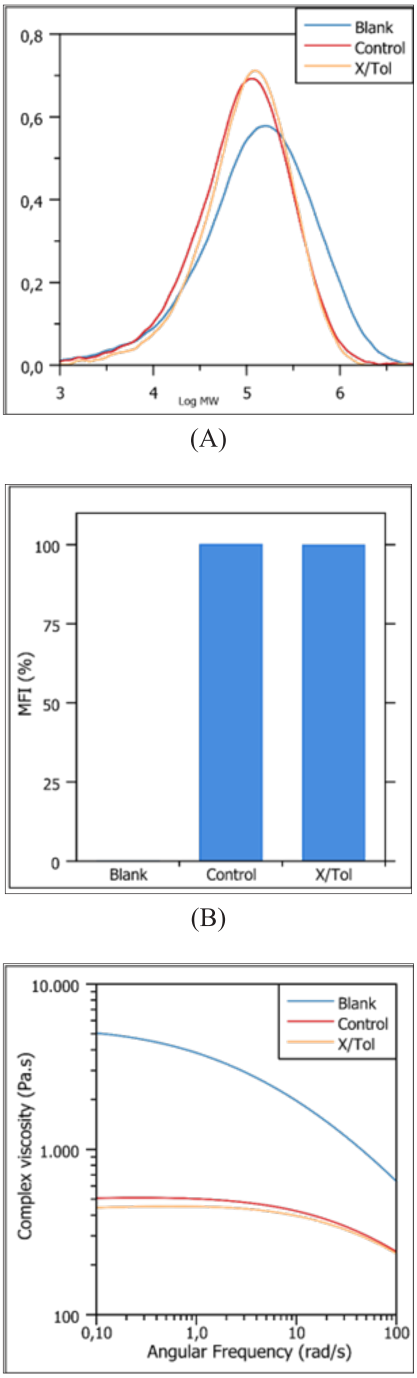

(A)

(B)

(C)

Figure 1: (A) GPC, (B) MFI, and (C) Rheology observations of X/Tol

Phenol

Because oxygen is more electronegative than carbon, it is inherently more stabilized. Even so, the position of the hydroxy adjacent to an aromatic ring will provide phenol with the additional stabilizing effect of the delocalized π-system of the ring. Therefore, phenol, like toluene, also falls into the second stabilization category defined in the introduction.

It is quite well understood that hindered phenols (butylated hydroxytoluene, Irganox 1010, Irganox B225, etc.) are antioxidizing agents, and are for that reason often added to polymer materials as additives (Iedema et al., 2011; Oromiehie et al., 2014; Schabron & Fenska, 1980; Wang et al., 2008). They scavenge for peroxy intermediates because the hydroxy hydrogen can be removed relatively easily, due to a large stabilization effect due to the aromatic conjugated π-system, as well as some hyperconjugation effects from the hindering side groups. This results in a phenoxy radical, which can react further in a number of ways to yield non-radical products (Gijsman, 2013). Even though side groups can have a strong electronic and steric effects, the phenoxy radical has been reported to be relatively long-lived (Ganapathi et al., 2001; Hermann et al., 2000). Its presence in a PP matrix may provide interesting insights.

Figure 4 implies quite clearly that phenol is able to suppress some of the degradation caused by the peroxide. The GPC results show a peak for X/Phen that lies somewhere in-between the control and the blank. This would suggest that there is still degradation, but that phenol somehow suppresses the extent of what the peroxide would have done alone. The MFI results show an index for X/Phen around 35%. Therefore, the MFI also suggests that some degradation still occurs, but to a lower extent than what the peroxide would have done alone.

The rheology results agree with what the GPC and MFI suggest. The X/Phen curve resides between the blank and the control, showing less shear-thinning than the blank, but more than the control. These results seem to indicate significant degradation, but to a lower extent compared to the peroxide control.

This observation requires an explanation. The β-scission mechanism consists effectively of 5 steps (Scheme 1):

1. The peroxide decomposes.
2. Once the peroxide has decomposed, the resulting radical abstracts a methine hydrogen.
3. The resulting macroradical rapidly breaks up, by jettisoning the entire chain from the β-position onwards, hence the term β-scission.
4. Alternatively, in a parallel process, the chain can be broken due to thermomechanical effects in the extruder.
5. The scheme propagates by a process of chain transfer, where severed radicals abstract a hydrogen from another chain.

The coagents (M) can interfere with the radical process in various ways (Scheme 2):

6. The coagent can interact with the radical initiator to prevent, or reduce the rate of, hydrogen abstraction.
7. The coagent may also interfere with the macroradical, by stripping it from its radical through hydrogen donation (7a) or by (reversibly) recombining with it (7b).
8. If it has more functionalities, it could serve as a coupling agent and facilitate branching.
9. The coagent could interfere with chain transfer in a similar way as the initiator.

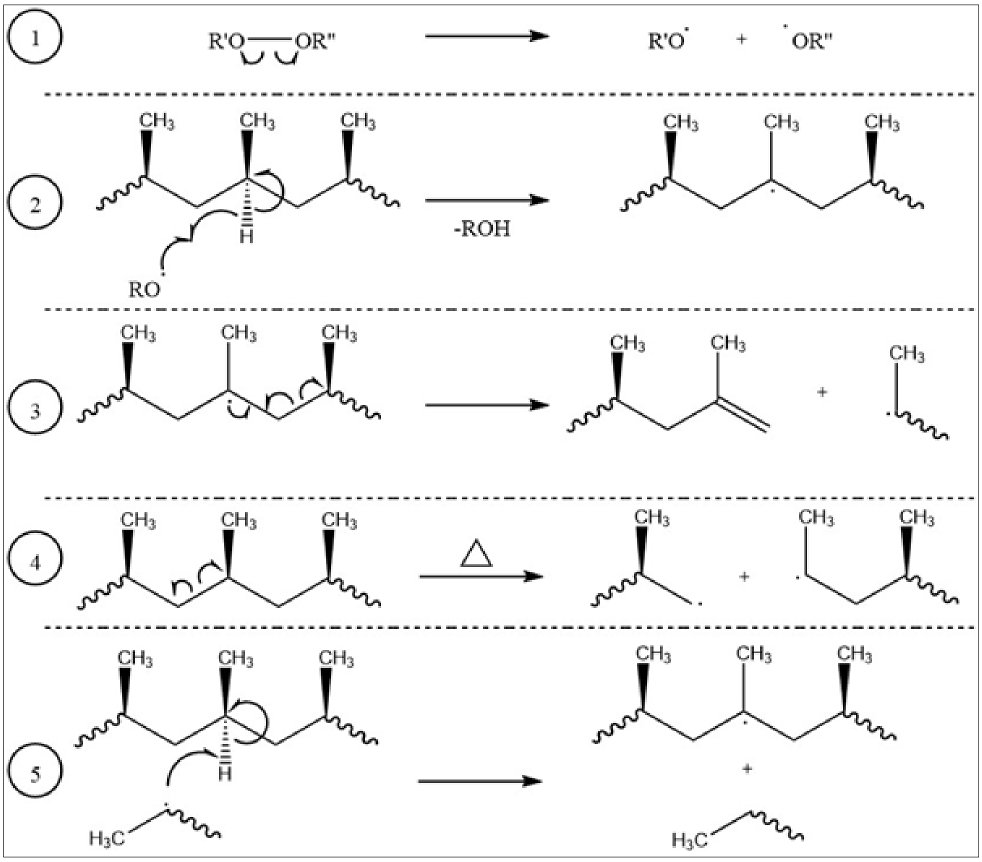

Scheme 1: Mechanism of β-scission

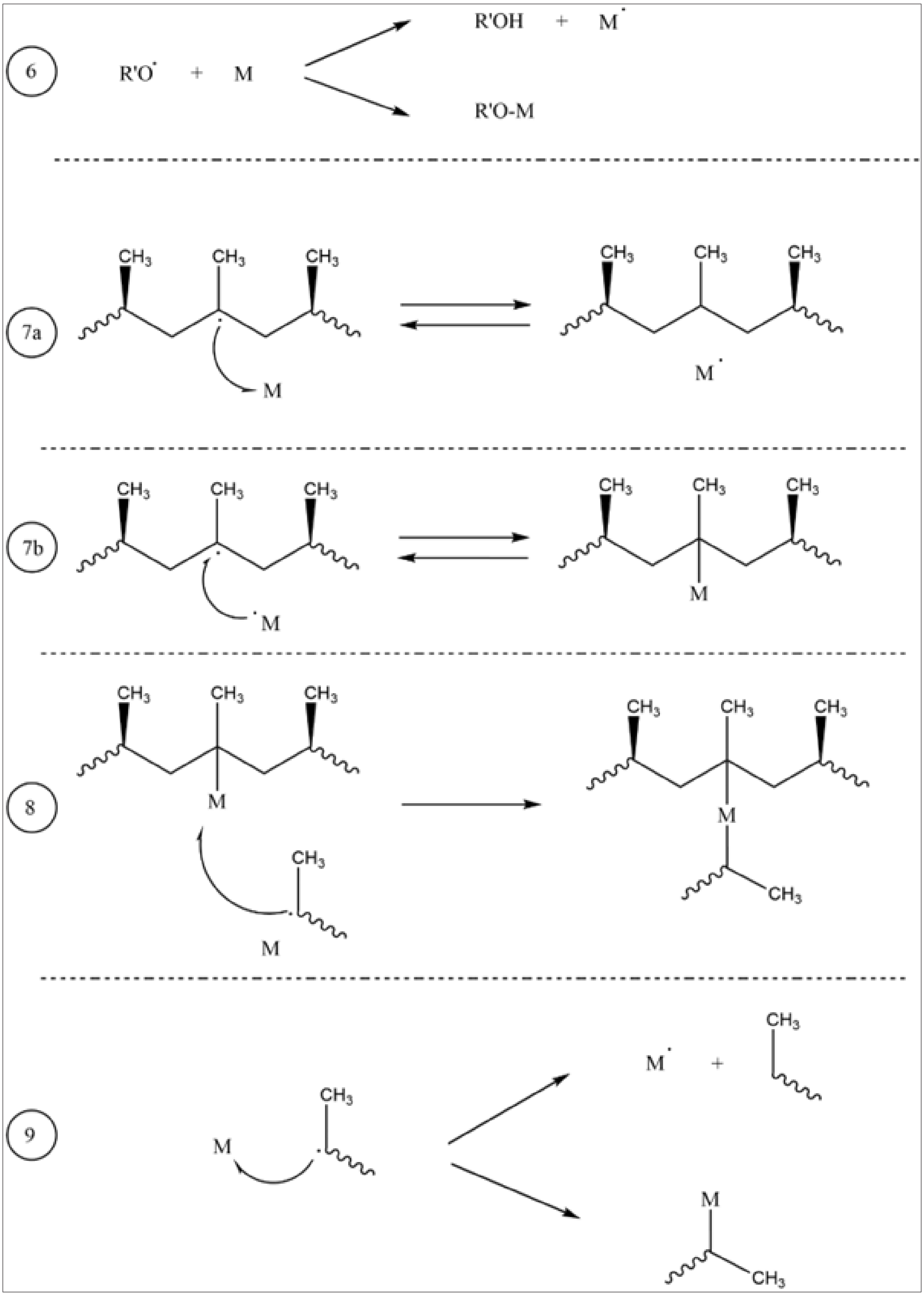

Scheme 2: Mechanism of coagent interference in β-scission

Either with or without the use of coagents, the radical mechanism works out through the usual termination pathways of disproportionation and recombination (not shown in the schemes).

The environment does have an influence on the stability of the radical. Half-life times can vary depending on the medium wherein it decomposes. The kinetic data provided by Nouryon in their brochure is different from the data provided to Tzoganakis et al for the same peroxide (Nouryon, n.d.; Tzoganakis et al., 1989).

Nevertheless, the amount of coagent added does not change the composition of the polymer matrix so substantially as to make it plausible that it can have such a drastic effect on the peroxide decomposition. As such, this is not the most likely explanation.

Another unlikely explanation is that the coagent would sufficiently stabilize the macroradical. Functionalization of PP is notoriously difficult because β-scission is usually too fast for anything to graft onto the backbone. In fact, during the modelling studies of the kinetics of peroxide degradation, the step of scission is usually presumed to be instantaneous, and these models seem to correlate with the experimental data rather well (Berzin et al., 2000; Iedema et al., 2001; Tzoganakis et al., 1989).

However, it would be easily verified if something grafted onto the PP backbone, which was checked by spectroscopic methods. Figure 5 shows the FTIR spectrum of X/Phen, where the spectrum is observed to be superimposable with both the blank and the control.

Phenol interference in steps 2 & 4 seem equally reasonable. Based on the X/Phen data, it is really difficult to state which of these two steps is more predominantly obstructed. However, from a technology perspective, this is irrelevant. The fact remains that phenol interferes in the degradation of PP by suppressing the effect that the peroxide would have in its absence.

Both due to the electronegativity of oxygen and the adjacent aromatic ring, phenol displays reasonable stabilization in case it loses its hydroxyl hydrogen, which may be taken by a radical. If the phenol molecules are poorly dispersed (Figure 3A), then phenol molecules might go about exchanging the radical between themselves, which would temporarily exclude the radical from participating in β-scission. However, the concentration of these phenol clusters would not be very high, due to it being poorly dispersed.

Alternatively, if phenol is well dispersed (Figure 3B), then its concentration in the system is effectively much higher, and the probability of phenol meeting a radical increases. However, phenol cannot pass the radical on to another phenol in the vicinity, because there are not as many as in a poorly dispersed system. This would increase the likelihood of phenol engaging in H-abstraction, and is only a temporary buffer between radical initiator and PP, and merely delays the inevitable β-scission.

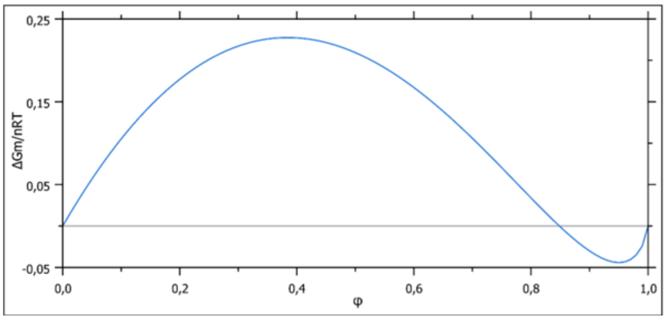

Figure 2: Free Gibbs energy of mixing between PP and phenol as function of the polymeric volume fraction

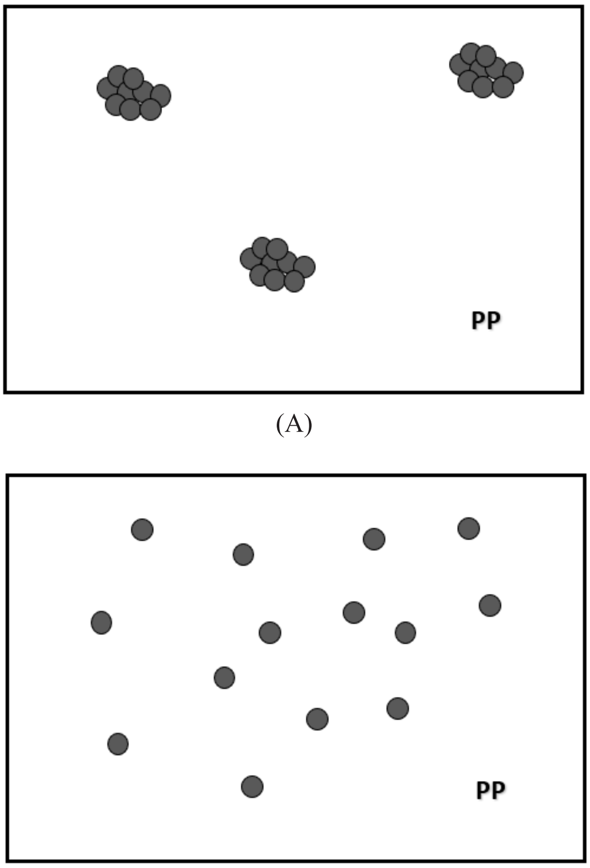

(A)

(B)

Figure 3: (A) poorly dispersed system, (B) well dispersed system

According to the structure-property relations as documented by Van Krevelen, the energy of mixing would be estimated to be at around -100 J, which is negative, and so spontaneous mixing can occur (van Krevelen, 2009). However, the number is relatively not so high as to justify the presumption of a well dispersed system. Figure 2 displays the energy of mixing normalized over the thermal components based on the calculation of the structure property relations as laid out by Van Krevelen. The current work operates at the far-right corner, where the volume fraction (φ) is close to 1. As such, the reality probably lies somewhere in the middle, where there are some phenol clusters, as well as some individual phenol molecules floating around the system.

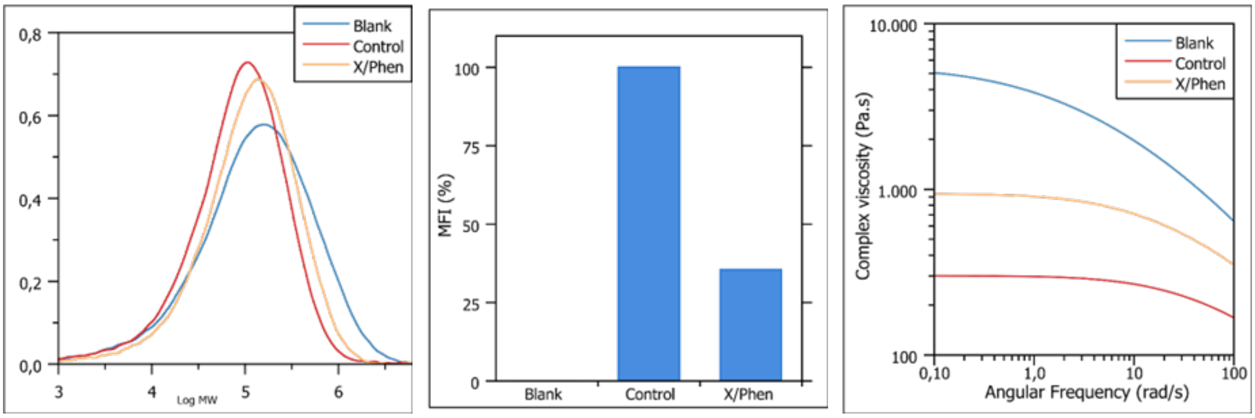

(A) (B) (C)

Figure 4: (A) GPC, (B) MFI, and (C) Rheology observations of X/Phen

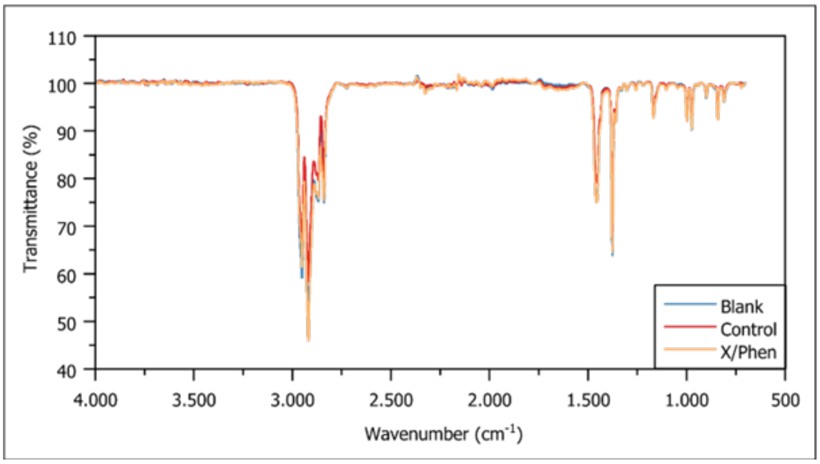

Figure 5: FTIR of X/Phen

Hydroquinone

Hydroquinone is a derivative of phenol, where it contains an additional hydroxy group attached to the benzyl ring in the para-formation. It is best known as a scavenging agent, both successful in free-radical scavenging (Kadoma & Fujisawa, 2000; Nakarada & Petković, 2018; Pozdeeva & Denisov, 2011), and cation-scavenging.(Duan et al., 2021) It even plays a role in a variety of biological processes (Casas et al., 1998; Hirakawa et al., 2002; Singh et al., 2014). However, a similar behaviour has been observed in the polymer industry (Chodák et al., 1987; Chodák & Matisová-Rychlá, 1986; Kadoma & Fujisawa, 2000).

Next to its scavenging effect, it must be observed that hydroquinone is a bifunctional agent, since it has two hydroxyl groups. As a result, it was found that hydroquinone can also act as a coupling agent between polymer chains. As such, it is a relevant agent both during polymerization and post-polymerization.

Given the tendency of PP to undergo degradation through beta-scission in the presence of free-radical agents, the effects of inhibition and branching might be interesting as a contribution to offer some competition to the mechanism. Long-chain branching, and to a higher extend even crosslinking, was found to be relevant predominantly at higher peroxide concentrations (Chodák et al., 1987; Chodák & Lazár, 1986; Chodák & Matisová-Rychlá, 1986; Tzoganakis et al., 1989). Since branching is not the intended result of this work, peroxide concentrations will be kept lower.

The GPC results show that the X/HQ peak virtually overlaps with the blank peak, which suggests that the influence of the peroxide has been completely nullified by hydroquinone. The MFI results show an index for X/HQ around 10, which is again very close to the value of the blank, thus reinforcing the observations of the GPC. The rheology results agree with what the GPC and MFI suggest. X/HQ overlaps with the blank, showing near identical zero-shear viscosity and shear-thinning behaviour.

It is not surprising that X/HQ shows a similar trend to X/Phen and goes even further. After all, the molar ratio remains the same, but hydroquinone has an additional hydroxy group per molecule. This results in the observation that under the conditions of this work, the presence of hydroquinone seems to fully nullify the effect of the peroxide. These results shed light on the observations made for X/Phen as well; in order for X/HQ to have the same value as the blank, there can have been effectively no degradation due to the peroxide, and so hydroquinone must have interrupted step 2 of Scheme 1. Since phenol relies on the same chemistry, a hydroxide group attached to an aromatic ring, it is likely that phenol will also have interrupted step 2. And like phenol, hydroquinone also shows no sign of grafting onto the PP backbone, as observed from the FTIR data (Figure 7).

As expected, the amounts of hydroquinone and peroxide used for this sample were too low to get some long-chain branches. We see from the rheology data (Figure 6C) that the curve for X/HQ overlaps very well with the curve for the linear blank PP. Additionally, the FTIR shows no grafting onto the backbone of hydroquinone; therefore, it could not have acted as coupling agent.

Since the X/HQ seems to be linear still, the overlapping values in Figure 6 indicate a suppression of degradation. These results reinforce hydroquinone’s function as free-radical scavenger.

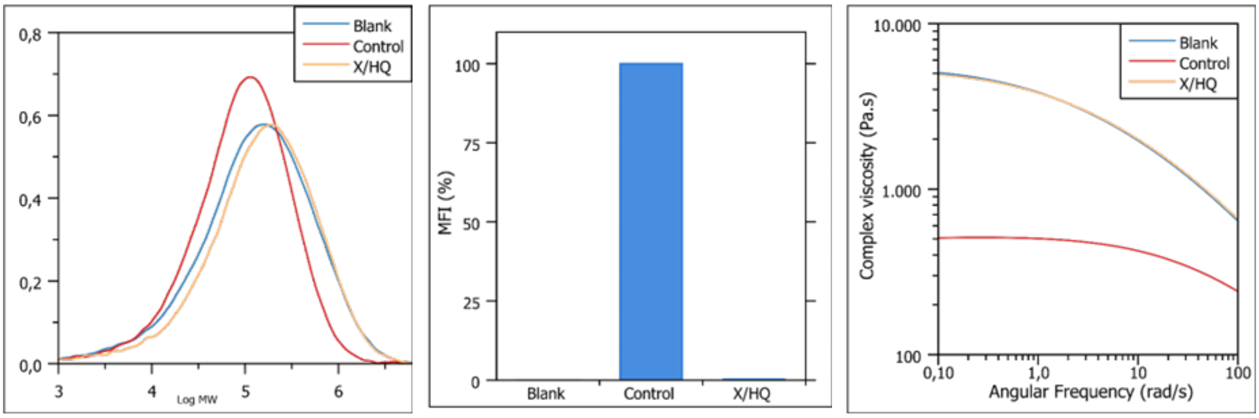

(A) (B) (C)

Figure 6: (A) GPC, (B) MFI, and (C) Rheology observations of X/HQ

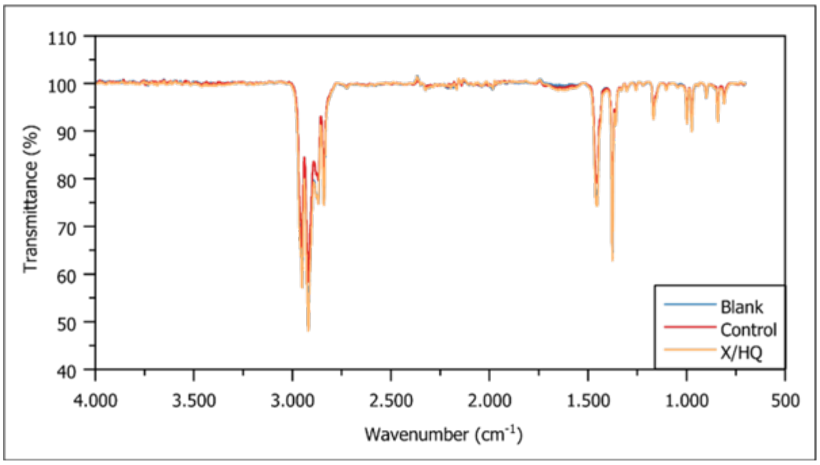

Figure 7: FTIR of X/HQ

Benzoquinone

Benzoquinone is a molecule that is closely related to hydroquinone. If both hydroxy hydrogens from Hydroquinone are removed, then what remains is a resonance structure of benzoquinone. Therefore, it is not surprising that benzoquinone exhibits similar properties in a system that is governed by radical reactions. If it is used in the quantities as described by Chodák (Chodák & Lazár, 1986), then we clearly see results that correlate with the properties of LCB-PP (Figure 8).

The GPC results show that for the usual peroxide concentration of 0.1 wt%, X/BQ overlaps with the blank PP fairly well, suggesting no degradation. The MFI backs this suggestion up by showing a value that is nigh identical to that of the blank, and also the rheology agrees with this conclusion.

However, if we use 10 times as much (10x BQ) then we see a slightly more pronounced shift of the MWD to the right, while also getting slightly broader. A widening MWD is a hint of branching, since it requires degradation followed by recombination of a broken PP chain and an unbroken PP chain; therefore, two chains of equal length would result in a smaller chain and a longer chain, hence widening the distribution (Lagendijk et al., 2001).

The MFI decreases substantially, to a value that is even lower than the blank, as well as the unmodified PP as received by Sabic. This is partly due to an increase in viscosity, as observed also by the rheology, as well as influences of a higher melt strength (Huovinen et al., 1997; Scheve et al., 1990; Su & Huang, 2011).

Furthermore, the shear thinning behaviour when using 10 times as much coagents is markedly more pronounced than that of the other samples. The viscosity also still increases very strongly at lower frequencies, where the other sample start to plateau. This behaviour is exactly what one would expect if long chain branching occurred, as seen by a comparison in Figure 8 with Daploy, an LCB-PP from Borealis.

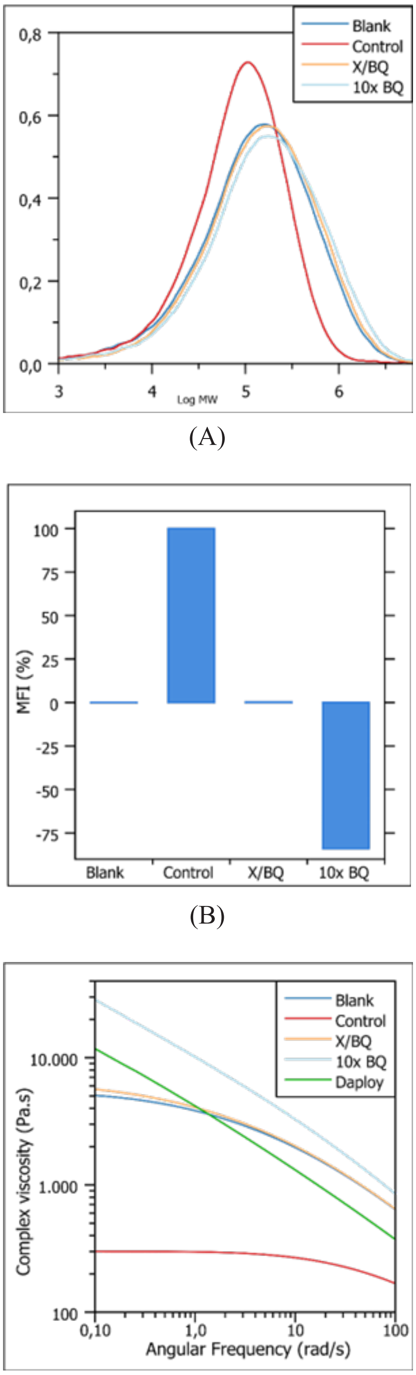

(A)

(B)

(C)

Figure 8: (A) GPC, (B) MFI, and (C) Rheology observations of X/BQ

NHPI

N-hydroxyphthalimide (NHPI) has been receiving a moderate amount of attention in literature, with particular interest into its function as organic catalyst for oxidation reactions (Hara et al., 2001; Liang & Jiao, 2017; Lin et al., 2012; Matsunaka et al., 1999; Minisci et al., 2004; Mo & Jensen, 2018; Opeida et al., 2011; Opeida et al., 2019). The operating mechanism is to generate the phthalimide-N-oxyl radical (PINO) from NHPI. As was reported in 2019, unlike other nitroxides such as TEMPO, PINO does not partake in reversible combination of radicals, but rather propagates the reaction scheme by abstracting a hydrogen elsewhere, and subsequently revert into NHPI.

However, that leaves the question of how it is initiated. Some reports involve a co-catalyst, e.g. cobalt or manganese, (Koshino et al., 2003; Minisci et al., 2004) and some claim that temperature and oxygen have an effect (Lin et al., 2012). Obviously the question becomes obsolete if a radical initiator is used.

PINO can abstract a hydrogen from both secondary and tertiary carbon atoms, but the tertiary carbon atom has a predominantly higher selectivity (Matsunaka et al., 1999). Presumably this is because of a higher effect of stabilization due to the inductive effect of electron donating groups surrounding this tertiary carbon.

Taking this into account, the results in Figure 9 should not come as a surprise. Whereas the GPC does not indicate that X/NHPI caused more degradation than the peroxide alone, both MFI and rheology seem to indicate a strong influence on behalf of NHPI as degradation accelerator. Looking at the mechanism in Scheme 1, it is clear as to why that is.

The peroxide initiator merely takes away an H-atom from the PP backbone. Once the radical is deposited on the polymer, PP becomes unstable and breaks. The β-scission step, therefore, is purely performed by PP, and all it requires is for something to take away an H-atom from a tertiary carbon. This is precisely the effect the NHPI has (Matsunaka et al., 1999; Opeida et al., 2019).

However, the GPC results do require a critical look, for if more degradation was truly occurring, this should show up at the GPC as well. One of the objections would be that the washing step may not have been entirely successful. NHPI has a reported melting point of 233°C, which means that it is around that point during MFI, but during rheology it should be firmly solid. During the reaction in the extruder, the temperature doesn't reach as high either, but the presence of $scCO_2$ might have dissolved some of the NHPI. It might be that it is purely a physical plasticising effect that reduces the viscosity owing to the low MW of NHPI. However, the FTIR did not detect any residual NHPI in the PP samples after washing (Figure 10).

Another point of contention between these three techniques is that GPC is performed in solution, whereas MFI and rheology are done in the melt. Melt processes are operated at higher temperatures than solution processes. It might be that the radical system is reactivated from a dormant state once temperatures increase, and the product is molten again. If that would be the case, then the rheology would not be stable over time, which is easily verified with a time sweep. However, the time sweep does not show a substantial drop over time (Figure 11).

The working theory is that NHPI might act as a nucleating agent which forms an aggregate of several chains around it which do not fully dissolve the PP. The GPC would be measuring such an aggregate as one big chain, while it is in fact multiple smaller ones. This would shift the distribution to higher values than it actually is. However, the fact that it would overlap almost perfectly with the control is unlikely to be mere coincidence.

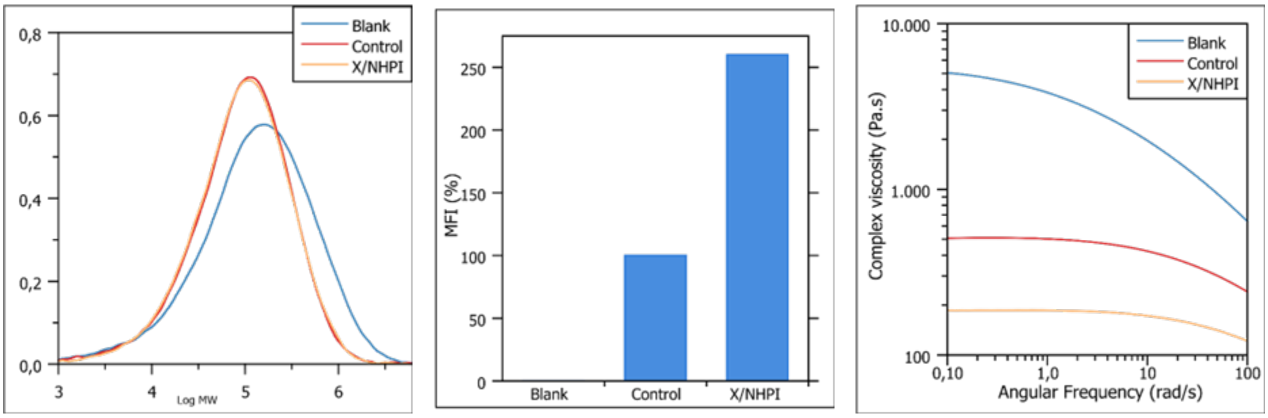

(A) (B) (C)

Figure 9: (A) GPC, (B) MFI, and (C) Rheology observations of X/NHPI

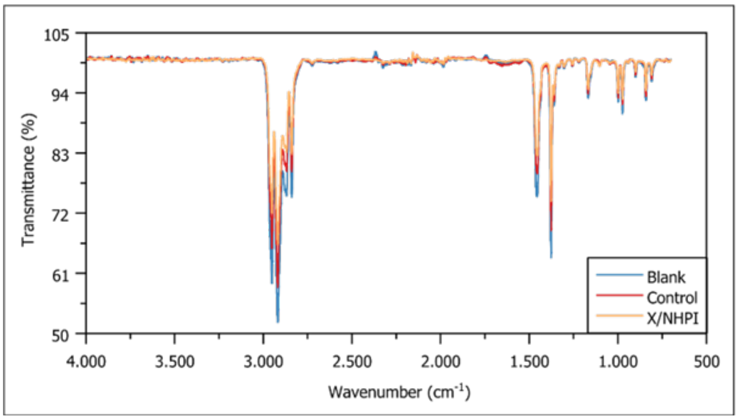

Figure 10: FTIR of X/NHPI

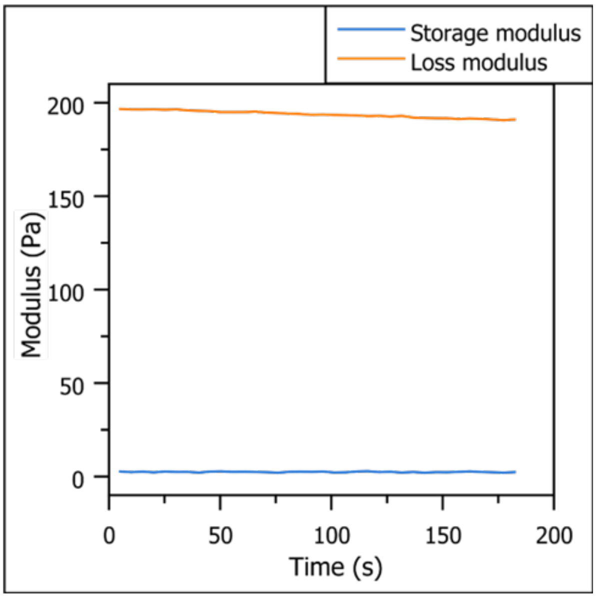

Figure 11: Time sweep X/NHPI

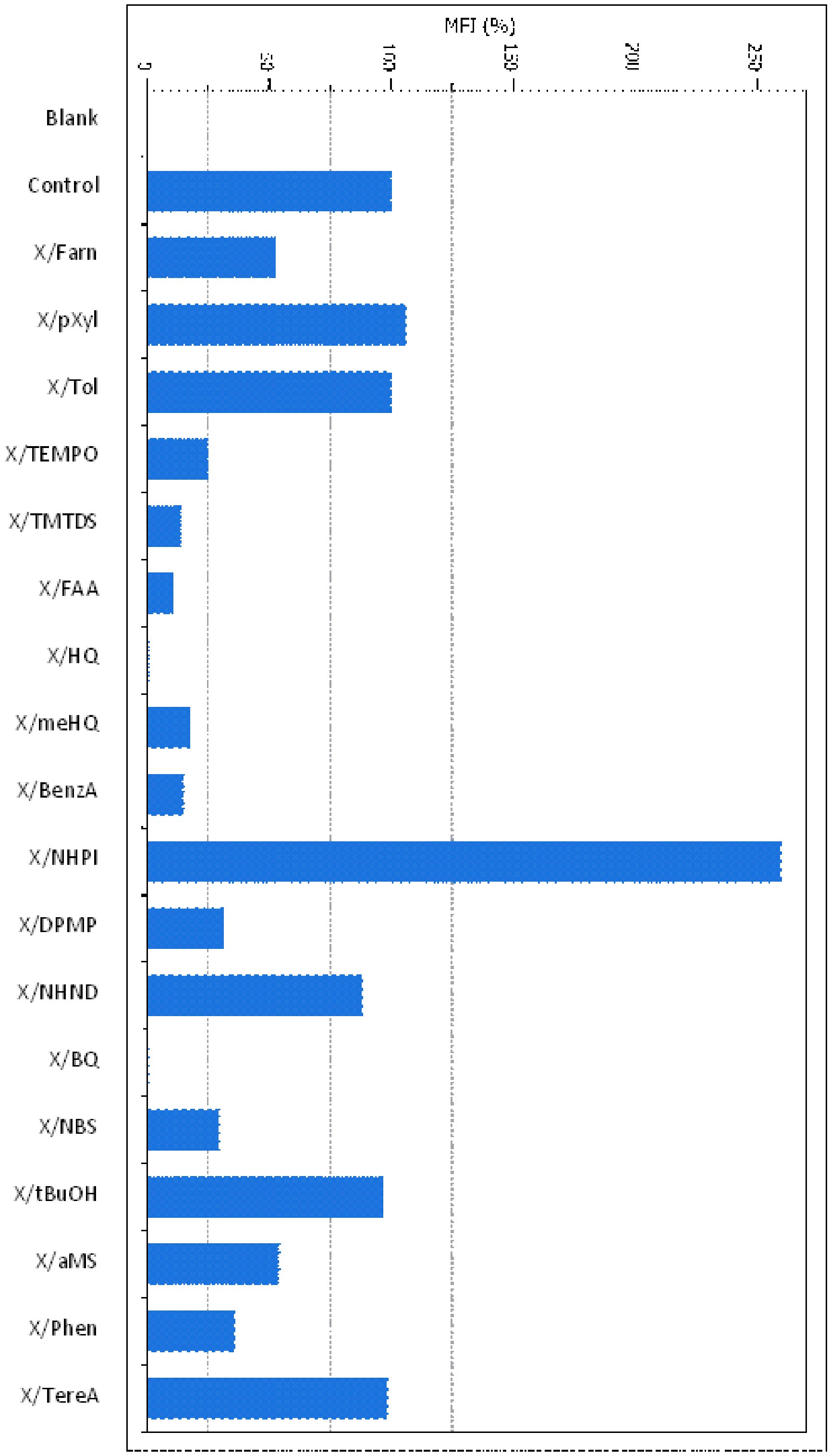

Figure 12: MFI results of all coagents, dotted lines are boundaries between categories.

X/Tol, X/Phen, X/HQ, and X/NHPI all showed different behaviour from each other, if only to the extent of their influence. All the other samples showed signs similar to one of those four, as is clearly demonstrated by looking at the MFI results (Figure 12). The similarities between X/BQ and X/HQ were already discussed. With the other values as well, it seems there are four overarching categories of behaviour:

1. Degradation enhancement: MFI exceeds 125% of the control.
2. Poor degradation suppression: MFI ranges from 75-125% of the control.
3. Decent degradation suppression: MFI ranges from 25-75% of the control.
4. Good degradation suppression: MFI less than 25% of the control.

It may very well be that the enhancement can be further subdivided into categories, but this work only found one coagent which might exhibit this type of behaviour.

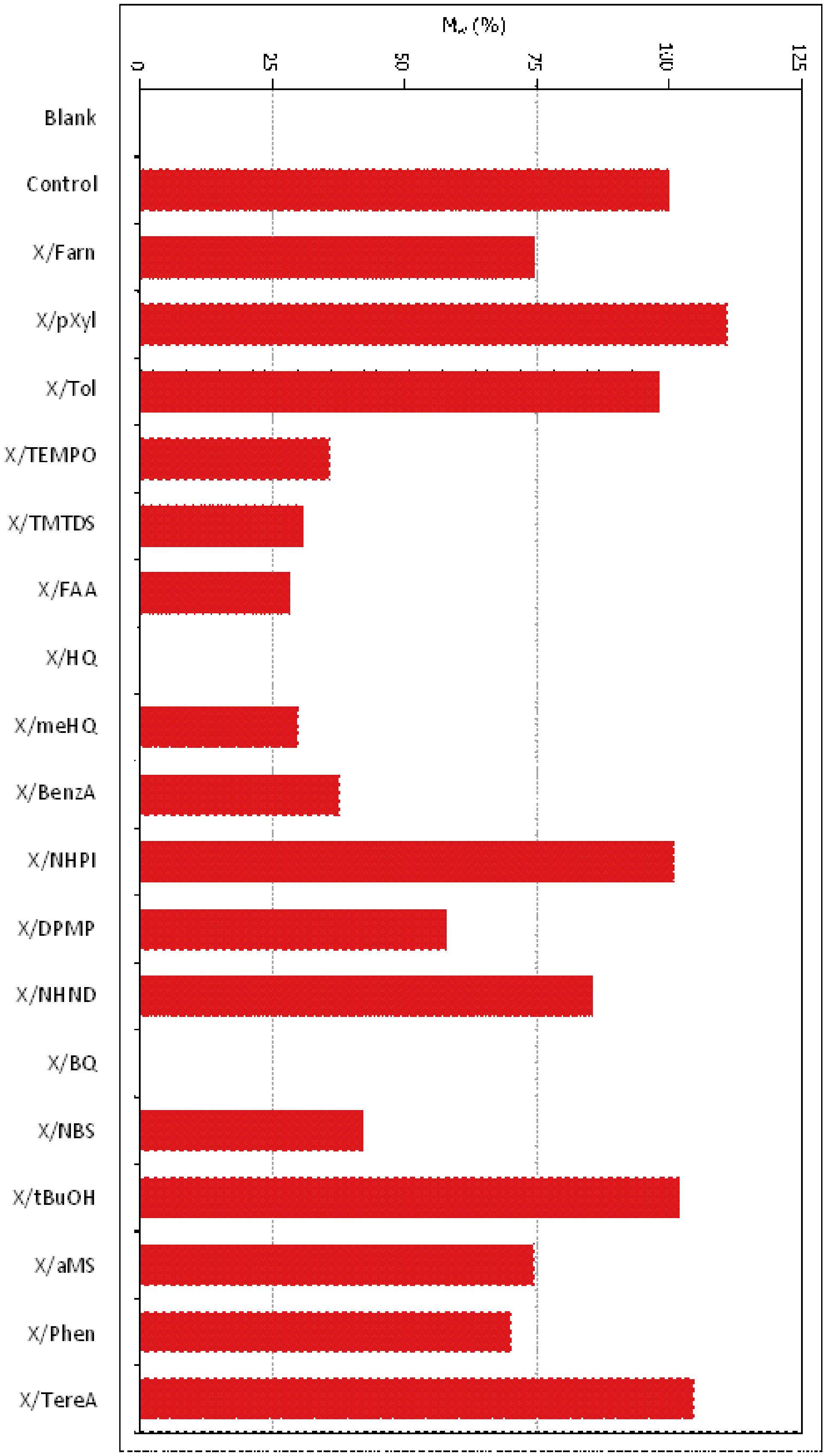

Figure 13: GPC results of all coagents, dotted lines are boundaries between categories.

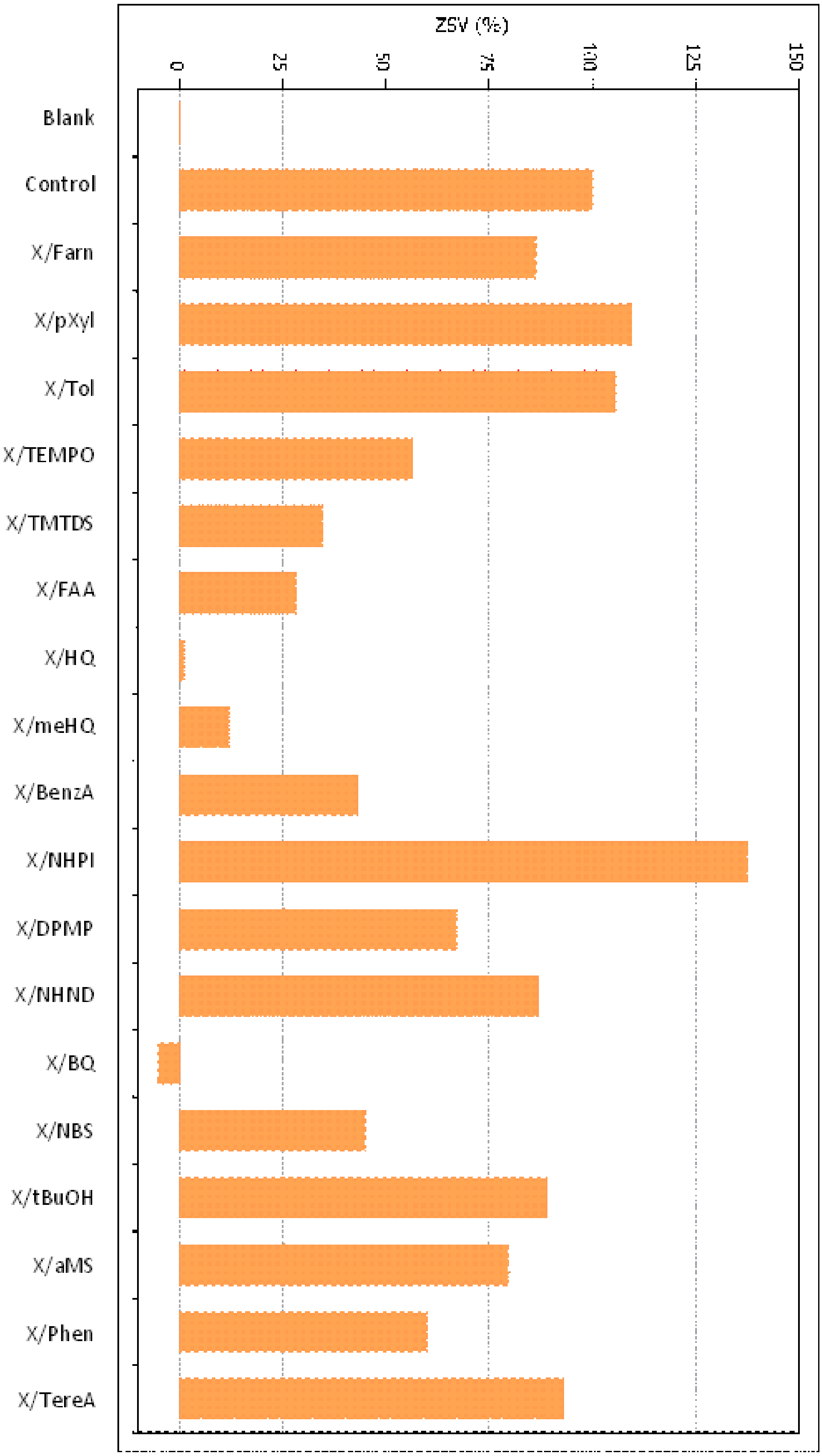

Figure 14: Rheology results of all coagents, dotted lines are boundaries between categories.

It stands to reason that degradation enhancement could also be divided into more categories, but this work found only one such coagent to exhibit this type of behaviour. Based on the data, the coagents seem to be able to be divided as such:

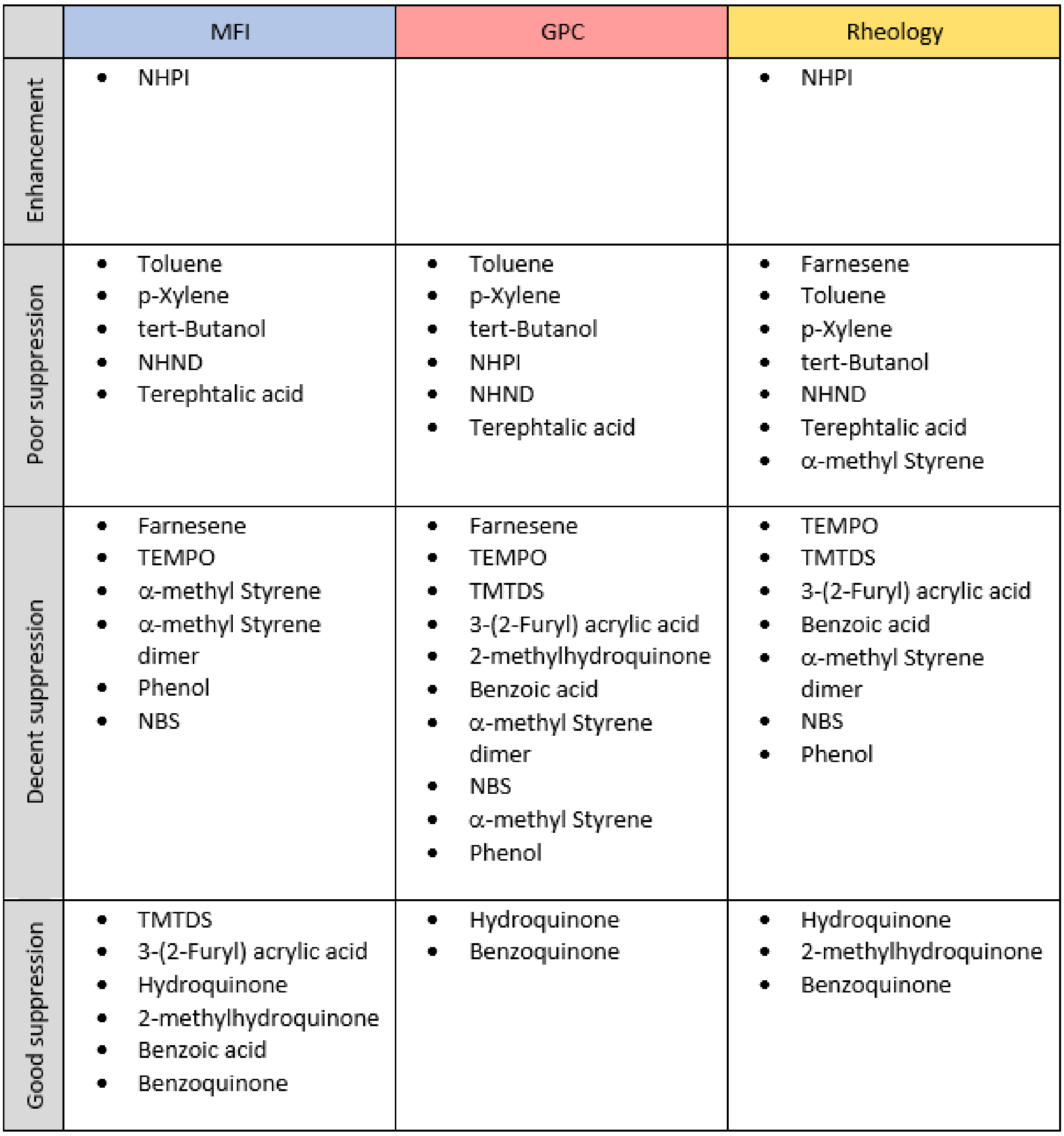

	MFI	GPC	Rheology
Enhancement	• NHPI		• NHPI
Poor suppression	• Toluene • p-Xylene • tert-Butanol • NHND • Terephtalic acid	• Toluene • p-Xylene • tert-Butanol • NHPI • NHND • Terephtalic acid	• Farnesene • Toluene • p-Xylene • tert-Butanol • NHND • Terephtalic acid • α-methyl Styrene
Decent suppression	• Farnesene • TEMPO • α-methyl Styrene • α-methyl Styrene dimer • Phenol • NBS	• Farnesene • TEMPO • TMTDS • 3-(2-Furyl) acrylic acid • 2-methylhydroquinone • Benzoic acid • α-methyl Styrene dimer • NBS • α-methyl Styrene • Phenol	• TEMPO • TMTDS • 3-(2-Furyl) acrylic acid • Benzoic acid • α-methyl Styrene dimer • NBS • Phenol
Good suppression	• TMTDS • 3-(2-Furyl) acrylic acid • Hydroquinone • 2-methylhydroquinone • Benzoic acid • Benzoquinone	• Hydroquinone • Benzoquinone	• Hydroquinone • 2-methylhydroquinone • Benzoquinone

Table 3: Coagent classification per analysis technique

The classifications in Table 3 overlap fairly well, considering that the correlation is fair (Figure 15) and the boundaries are arbitrary. Regardless, it is still a useful heuristic in a broad sense. The benzylic position in Toluene and p-xylene always shows poor degradation suppression, whereas hydroquinone and benzoquinone always show good degradation suppression, with phenol and benzoic acid acting somewhere in between. This clearly suggests that the hydroxy and carbonyl group directly adjacent to an aromatic ring show excellent stabilization to participate in the radical system, whereas the benzylic position seems to be inactive. The most inconsistent group seems to be the nitroxide, which ranges from decent suppression to enhancement, depending on the chemical structure of the rest of the molecule.

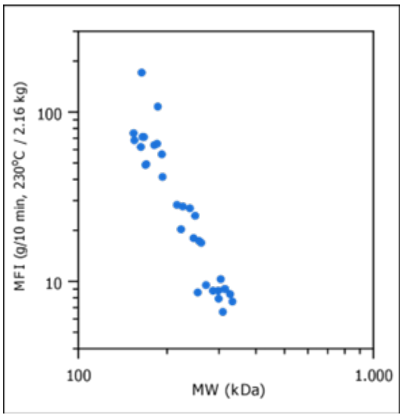

(A) Correlation between MFI and Mw (weight average MW): 0.90

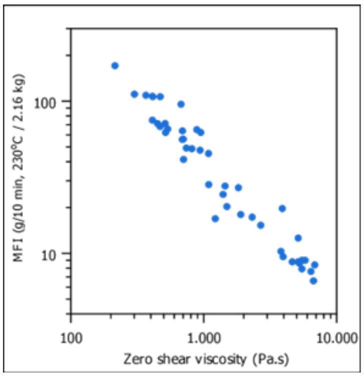

(B) Correlation between MFI and zero-shear viscosity: 0.97

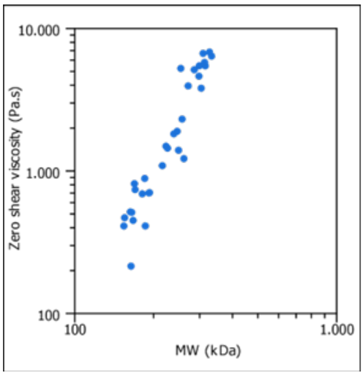

(C) Correlation between zero-shear viscosity and M_w (weight average MW): 0.88

Figure 15: Correlation between analysis techniques GPC, MFI, and rheology

The FTIR spectra all fail to show active grafting, as they are all superimposable with the reference spectra, without any indication of the groups one would expect to appear in the case of functionalization.

Regardless, this would not necessarily eliminate the contribution of reaction 7a in Scheme 2. Therefore, NMR spectra were taken in addition to see if the stereoregularity of the reference PP was changed. However, the NMR spectra were also superimposable (Figure 16), with the exception of NBS. This comes as no surprise, given that the tendency of NBS to facilitate rapid chain transfer has been reported before. This is also reflected in the crystallinity, which is why a DSC (Figure 17) was taken to observe the thermal properties of the PP samples before and after treatment with the coagents (Henry et al., 2009; Listner, 1970b; Listner 1970a; Passaglia et al., 2014).

The DSC has an error of around 5%. Figure 17 shows a dotted line at the blank value of 100 J/g. There are two more dotted lines which represent the 5% boundary. Anything within these two lines does not fall outside of experimental error, and is for all intends and purposes virtually the same. Only NBS breaks through this barrier, although not as substantially as one might have thought based on the aforementioned literature.

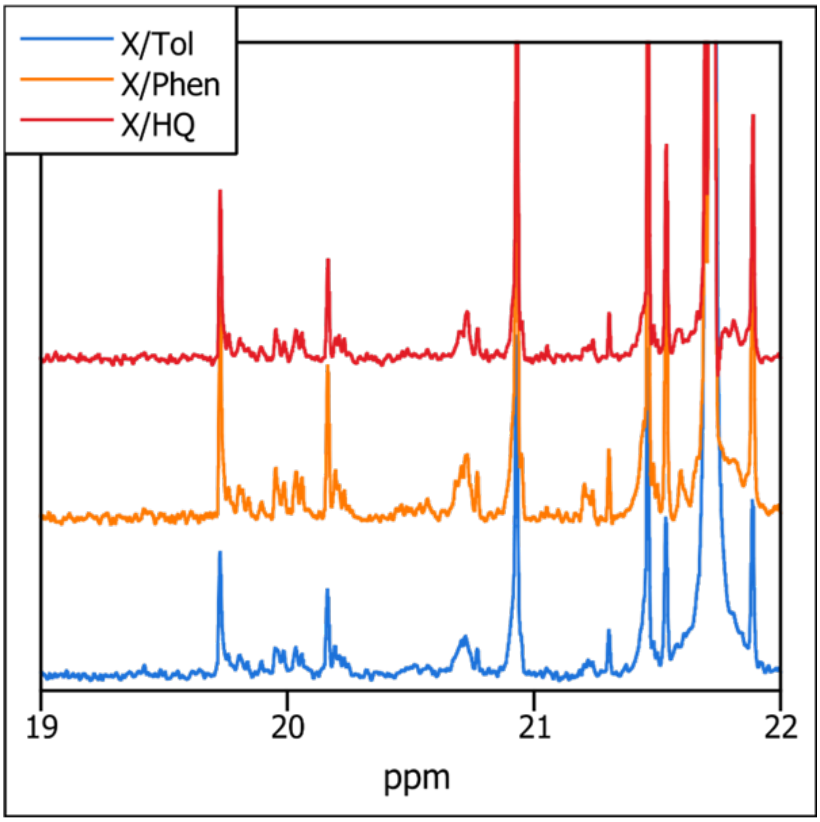

Figure 16: ^{13}C-NMR results of X/Tol, X/Phen, and X/HQ at the tertiary carbon region

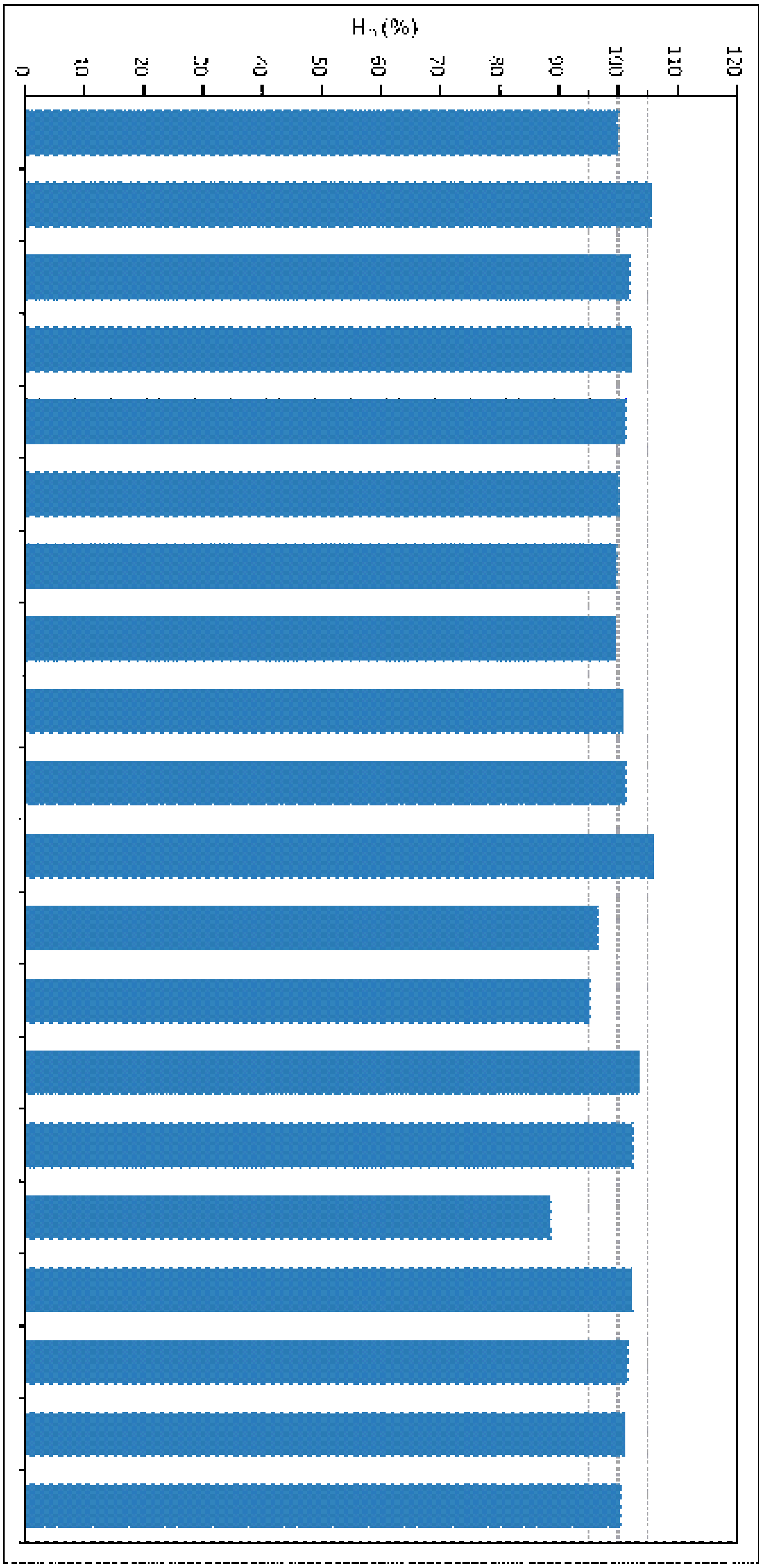

Figure 17: Melt enthalpy results of all coagents as measured by DSC

Conclusion

The degradation behaviour of PP by Trigonox 101 was studied in the presence of a variety of coagents. A substantial number of these coagents did not seem to participate in the reaction, such as those with only a benzylic position, e.g. toluene and xylene. These showed little to no suppression of the degradation, while also not showing functionalization on FTIR, NMR, and the thermal properties weren't changed as far as DSC is concerned.

These techniques showed that another portion of coagents, such as those with heteroatoms attached to an aromatic ring, did suppress the degradation to some extent, but no more than that under the operation conditions applied. A third class seemed most potent in their ability to supress the degradation to the point where the peroxide had seemingly no effect at all. Upon higher concentrations, some of these coagents proved to be able to undergo long-chain branching.

A fourth category may have been identified where NHPI acted as an accomplice to the peroxide, and degraded the PP to an even higher extend than Trigonox 101 would have done alone. Other nitroxides did not join in this category. TEMPO showed signs of decent degradation suppression, whereas NHND seemed to be hardly involved in the scheme at all.

Acknowledgments

The authors would like to thank SNN and the Province of Groningen for funding through the European Fund for Regional Development platform. They furthermore are grateful for the insights offered by Klaas Remerie, Frits Zandvoort, Waldo Beek, Gert Boven, Rob Duchateau, and Daniele Parisi.

References

1. Huovinen, P., Harlin, A., Jääskeläinen, P., Karbasi, A. & Manner, N. (1997). High melt strength polypropylene (Patent US6875826B1). Borealis Technology Oy.
2. Scheve, J. B., Mayfield, J. W. & DeNicola, A. J. Jr. (1998). High melt strength, propylene polymer, process for making it, and use thereof (Patent US5731362A). Retrieved from https://patents.google.com/patent/US5731362A/en
3. Dorscht, B. M. & Tzoganakis, C. (2002). Reactive extrusion of polypropylene with supercritical carbon dioxide: Free radical grafting of Maleic anhydride. *Journal of Applied Polymer Science, 87*(7), 1116–1122. DOI: https://doi.org/10.1002/app.11561
4. Liu, T., Hu, G. H., Tong, G. S., Zhao, L., Cao, G. P. & Yuan, W. K. (2005). Supercritical carbon dioxide assisted solid-state grafting process of maleic anhydride onto polypropylene. *Industrial and Engineering Chemistry Research, 44*(12), 4292–4299. DOI: https://doi.org/10.1021/ie0501428
5. Oromiehie, A., Ebadi-Dehaghani, H. & Mirbagheri, S. (2014). Chemical Modification of Polypropylene by Maleic Anhydride: Melt Grafting, Characterization and Mechanism. *International Journal of Chemical Engineering and Applications, 5*(2), 117–122. DOI: https://doi.org/10.7763/ijcea.2014.v5.363
6. Berzin, F., Vergnes, B., Dufossé, P. & Delamare, L. (2000). Modeling of peroxide initiated controlled degradation of polypropylene in a twin screw extruder. *Polymer Engineering and Science, 40*(2), 344–356. DOI: https://doi.org/10.1002/pen.11168
7. Iedema, P. D., Willems, C., Van Vliet, G., Bunge, W., Mutsers, S. M. P. & Hoefsloot, H. C. J. (2001). Using molecular weight distributions to determine the kinetics of peroxide-induced degradation of polypropylene. *Chemical Engineering Science, 56*(12), 3659–3669. DOI: https://doi.org/10.1016/S0009-2509(01)00054-9
8. Tzoganakis, C., Hamielec, A. E., Tang, Y. & Vlachopoulos, J. (1989). Controlled degradation of polypropylene: A comprehensive experimental and theoretical investigation. *Polymer-Plastics Technology and Engineering, 28*(3), 319–350. DOI: https://doi.org/10.1080/03602558908048602
9. Brown, W., Rajbenback, L. & Eirich, F. R. (1962). Peroxide Decomposition and Cage Effect. *The Journal of Physical Chemistry, 66*(9), 1591–1595. Retrieved from https://pubs.acs.org/sharingguidelines
10. Picchioni, F. (2014). Supercritical carbon dioxide and polymers: An interplay of science and technology. *Polymer International, 63*(8), 1394–1399. DOI: https://doi.org/10.1002/pi.4722
11. Lei, Z., Ohyabu, H., Sato, Y., Inomata, H. & Smith, R. L. (2007). Solubility, swelling degree and crystallinity of carbon dioxide-polypropylene system. *Journal of Supercritical Fluids, 40*(3), 452–461. DOI: https://doi.org/10.1016/j.supflu.2006.07.016
12. Sato, Y., Fujiwara, K., Takikawa, T., Sumarno, Takishima, S. & Masuoka, H. (1999). Solubilities and diffusion coefficients of carbon dioxide and nitrogen in polypropylene, high-density polyethylene, and polystyrene under high pressures and temperatures. *Fluid Phase Equilibria, 162*(1–2), 261–276. DOI: https://doi.org/10.1016/S0378-3812(99)00217-4
13. Busico, V., Cipullo, R., Mingione, A. & Rongo, L. (2016). Accelerating the Research Approach to Ziegler-Natta Catalysts. *Industrial and Engineering Chemistry Research, 55*(10), 2686–2695. DOI: https://doi.org/10.1021/acs.iecr.6b00092
14. Busico, V. & Cipullo, R. (2001). Microstructure of polypropylene. *Progress in Polymer Science, 26*(3), 443–533. DOI: https://doi.org/10.1016/S0079-6700(00)00046-0
15. Seavey, K. C., Liu, Y. A., Khare, N. P., Bremner, T. & Chen, C. C. (2003). Quantifying relationships among the molecular weight distribution, non-Newtonian shear viscosity, and melt index for linear polymers. *Industrial and Engineering Chemistry Research, 42*(21), 5354–5362. DOI: https://doi.org/10.1021/ie021003i
16. Wu, W., Jiang, W., Fu, Z., Xiao, J., Yuan, D. & Xing, C. (2023). Comparison of Dynamic and Steady Viscosity in High-Viscosity Modified Asphalt Binder and Analysis of Its Zero Shear Viscosity Test Methods. *Journal of Materials in Civil Engineering, 36*(2), 04023574. DOI: https://doi.org/10.1061/JMCEE7.MTENG-16635
17. Agilent Technologies. (2015). An Introduction to

Gel Permeation Chromatography and Size Exclusion Chromatography. Retrieved from https://www.agilent.com/cs/library/primers/Public/5990-6969EN%20GPC%20SEC%20Chrom%20Guide.pdf

18. Boyron, O., Cancelas, A. J., Taam, M., Boisson, C. & McKenna, T. (2017). A new straightforward method for measuring xylene soluble for high impact polypropylene. *Canadian Journal of Chemical Engineering, 95*(5), 939–943. DOI: https://doi.org/10.1002/cjce.22735
19. Shenoy, M. A. & Patil, M. (2010). Studies in reduction of molecular weight of polypropylene. *Polymer Science - Series B, 52*(3–4), 174–183. DOI: https://doi.org/10.1134/S1560090410030073
20. Wang, J., Wang, D., Du, W., Zou, E. & Dong, Q. (2009). Synthesis of functional polypropylene via Solid-phase grafting soft vinyl monomer and its mechanism. *Journal of Applied Polymer Science, 113*(3), 1803–1810. DOI: https://doi.org/10.1002/app.30179
21. Iedema, P. D., Remerie, K., van der Ham, M., Biemond, E. & Tacx, J. (2011). Controlled peroxide-induced degradation of polypropylene in a twin-screw extruder: Change of molecular weight distribution under conditions controlled by micromixing. *Chemical Engineering Science, 66*(22), 5474–5486. DOI: https://doi.org/10.1016/j.ces.2011.06.071
22. Schabron, J. F. & Fenska, L. E. (1980). Determination of BHT, Irganox 1076, and Irganox 1010 Antioxidant Additives in Polyethylene by High Performance Liquid Chromatography. *Analytical Chemistry, 52*(9), 1411–1415. DOI: https://doi.org/10.1021/AC50059A009
23. Wang, X., Zhang, Y., Liu, B. & Du, Z. (2008). Crystallization behavior and crystal morphology of linear/long chain branching polypropylene blends. *Nature.Com, 40*(5), 450–454. DOI: https://doi.org/10.1295/polymj.PJ2007195
24. Gijsman, P. (2013). Polymer Stabilization. In M. Kutz (Ed.), Handbook of Environmental Degradation of Materials: Second Edition (2nd ed., pp. 673–714). Elsevier Inc. DOI: https://doi.org/10.1016/C2010-0-66227-4
25. Ganapathi, M. R., Naumov, S., Hermann, R. & Brede, O. (2001). Nucleophilic effects on the deprotonation of phenol radical cations. *Chemical Physics Letters*, 337, 335–340. Retrieved from www.elsevier.nl/locate/cplett
26. Hermann, R., Naumov, S., Mahalaxmi, G. R. & Brede, O. (2000). Stability of phenol and thiophenol radical cations-interpretation by comparative quantum chemical approaches. *Chemical Physics Letters*, 324, 265–272. Retrieved from www.elsevier.nlrlocatercplett
27. Nouryon. (n.d.). Initiators for Thermoplastics. Retrieved 4 July 2020, from https://www.nouryon.com/globalassets/inriver/resources/brochure-initiators-for-thermoplastics-en_us.pdf
28. van Krevelen, D. W. (2009). Properties of Polymers: Their Correlation with Chemical Structure; Their Numerical Estimation and Prediction from Additive Group Contributions (K. te Nijenhuis, Ed.; 4th ed.). Elsevier. Retrieved from https://www.unpa.edu.mx/~aramirez/propiedades%20de%20polimeros.pdf
29. Kadoma, Y. & Fujisawa, S. (2000). Kinetic evaluation of reactivity of bisphenol A derivatives as radical scavengers for methacrylate polymerization. *Biomaterials*,21 (21), 2125-2130. DOI: https://doi.org/10.1016/S0142-9612(00)00088-0
30. Nakarada, Đ. & Petković, M. (2018). Mechanistic insights on how hydroquinone disarms OH and OOH radicals. *International Journal of Quantum Chemistry, 118*(4). DOI: https://doi.org/10.1002/qua.25496
31. Pozdeeva, N. N. & Denisov, E. T. (2011). Mechanism of hydroquinone-inhibited oxidation of acrylic acid and methyl methacrylate. *Kinetics and Catalysis, 52*(4), 506–512. DOI: https://doi.org/10.1134/S0023158411040136
32. Duan, S., Uragami, C., Horiuchi, K., Hino, K., Wang, X. F., Sasaki, S. ichi, Tamiaki, H. & Hashimoto, H. (2021). Hydroquinone redox mediator enhances the photovoltaic performances of chlorophyll-based bio-inspired solar cells. *Communications Chemistry, 4*(1). DOI: https://doi.org/10.1038/s42004-021-00556-5
33. Casas, D. A., Prrfa-Alvarez, S. I. & Giulierri, A. M. (1998). Biotransformation of hydroquinone by hairy roots of Brugmansia candida and effect of sugars and free-radical scavengers. *Applied Biochemistry and Biotechnology, 69*(2), 127–136. DOI: https://doi.org/10.1007/bf02919394
34. Hirakawa, K., Oikawa, S., Hiraku, Y., Hirosawa, I. & Kawanishi, S. (2002). Catechol and hydroquinone have different redox properties responsible for their differential DNA-damaging ability. *Chemical Research in Toxicology, 15*(1), 76–82. DOI: https://doi.org/10.1021/tx010121s
35. Singh, J. V., Saurabh, M., Ajeet, S. & Raj, K. (2014). Free Radical Scavenging and Radioprotective Activities of Hydroquinone in Vitro. *Journal of Radioprotection Research, 2*(3), 37. DOI: https://doi.org/10.12966/jrr.09.01.2014
36. Chodák, I., Romanov, A., Rätzsch, M. & Haudel, G. (1987). Influence of the additives on polyethylene crosslinking initiated by peroxides. *Acta Polymerica, 38*(12), 672–674. DOI: https://doi.org/10.1002/actp.1987.010381208
37. Chodák, I. & Matisová-Rychlá, L. (1986). Thermooxidative stability of crosslinked polypropylene. *Polymer Degradation and Stability, 16*(3), 213–220. DOI: https://doi.org/10.1016/0141-3910(86)90027-3
38. Chodák, I. & Lazár, M. (1986). Peroxide-initiated crosslinking of polypropylene in the presence of p-benzoquinone. *Journal of Applied Polymer Science, 32*(6), 5431–5437. DOI: https://doi.org/10.1002/app.1986.070320615
39. Lagendijk, R. P., Hogt, A. H., Buijtenhuijs, A. & Gotsis, A. D. (2001). Peroxydicarbonate modification of polypropylene and extensional flow properties. In Polymer (Vol. 42, Issue 25). DOI: https://doi.org/10.1016/S0032-3861(01)00553-5
40. Scheve, J. B., Mayfield, J. W. & DeNicola, A. J. Jr. (1990). High melt strength, propylene polymer, process for making it, and use thereof (Patent US4916198A). Retrieved from https://patents.google.com/patent/US4916198A/en
41. Su, F. H. & Huang, H. X. (2011). Supercritical carbon dioxide-assisted reactive extrusion for preparation long-chain branching polypropylene and its rheology. *Journal*

of Supercritical Fluids, 56(1), 114–120. DOI: https://doi.org/10.1016/j.supflu.2010.12.001

42. Hara, T., Iwahama, T., Sakaguchi, S. & Ishii, Y. (2001). Catalytic oxyalkylation of alkenes with alkanes and molecular oxygen via a radical process using N-hydroxyphthalimide. *Journal of Organic Chemistry, 66*(19), 6425–6431. DOI: https://doi.org/10.1021/jo0157977
43. Liang, Y. F. & Jiao, N. (2017). Oxygenation via C-H/C-C Bond Activation with Molecular Oxygen. *Accounts of Chemical Research, 50*(7), 1640–1653. DOI: https://doi.org/10.1021/acs.accounts.7b00108
44. Lin, R., Chen, F. & Jiao, N. (2012). Metal-free, NHPI catalyzed oxidative cleavage of C-C double bond using molecular oxygen as oxidant. *Organic Letters, 14*(16), 4158–4161. DOI: https://doi.org/10.1021/ol3018215
45. Matsunaka, K., Iwahama, T., Sakaguchi, S. & Ishii, Y. (1999). A Remarkable Effect of Quaternary Ammonium Bromide for the N-Hydroxyphthalimide-Catalyzed Aerobic Oxidation of Hydrocarbons. *TETRAHEDRON LETTERS, 40*(11), 2165-2168. DOI: https://doi.org/10.1016/S0040-4039(99)00139-2
46. Minisci, F., Recupero, F., Cecchetto, A., Gambarotti, C., Punta, C., Paganelli, R., Pedulli, G. F. & Fontana, F. (2004). Solvent and temperature effects in the free radical aerobic oxidation of alkyl and acyl aromatics catalysed by transition metal salts and N-hydroxyphthalimide: New processes for the synthesis of p-hydroxybenzoic acid, diphenols, and dienes for liquid crystals and cross-linked polymers. *Organic Process Research and Development, 8*(2), 163–168. DOI: https://doi.org/10.1021/op034137w
47. Mo, Y. & Jensen, K. F. (2018). Continuous N-Hydroxyphthalimide (NHPI)-Mediated Electrochemical Aerobic Oxidation of Benzylic C−H Bonds. *Chemistry - A European Journal, 24*(40), 10260–10265. DOI: https://doi.org/10.1002/chem.201802588
48. Opeida, I. A., Kompanets, M. A., Papayanina, E. S. & Kushch, O. V. (2011). Action of N-hydroxyphthalimide on Chain Stereoregularity in the Radical Polymerization of Methyl Methacrylate. *Theoretical and Experimental Chemistry, 47*(1), 30–35. DOI: http://dx.doi.org/10.1007/s11237-011-9180-3
49. Opeida, I. O., Kushch, O. V., Kompanets, M. O., Litvinov, Y. E., Zosenko, O. O. & Shendrik, A. N. (2019). The Oxidative Polymerization of Vinyl Monomers in the Presence of N-Hydroxyphthalimide. *ChemistrySelect, 4*(40), 11826–11832. DOI: https://doi.org/10.1002/slct.201902597
50. Koshino, N., Cai, Y. & Espenson, J. H. (2003). Kinetic study of the phthalimide N-oxyl (PINO) radical in acetic acid. Hydrogen abstraction from C-H bonds and evaluation of O-H bond dissociation energy of N-hydroxyphthalimide. *Journal of Physical Chemistry A, 107*(21), 4262–4267. DOI: https://doi.org/10.1021/jp0276193
51. Henry, G. R. P., Drooghaag, X., Vandeuren, M., Sclavons, M., Schanck, A., Devaux, J., Carlier, V. & Marchand-Brynaert, J. (2009). Controlled reduction of polypropylene lsotacticity and crystallinity by epimerization during reactive processing. *Journal of Polymer Science, Part A: Polymer Chemistry, 47*(18), 4505–4518. DOI: https://doi.org/10.1002/pola.23504
52. Listner, G. J. (1970b). Sterically Rearranged Polymers (Patent US3515687).
53. Listner, G. J. (1970a). Novel polypropylene having isotactic-randiotactic structure (Patent US3511824). Johnson & Johnson. Retrieved from https://worldwide.espacenet.com/patent/search/family/024521399/publication/US3511824A?q=US3511824
54. Passaglia, E., Coiai, S., Cicogna, F. & Ciardelli, F. (2014). Some recent advances in polyolefin functionalization. *Polymer International, 63*(1), 12–21. DOI: https://doi.org/10.1002/pi.4598